Atmos. Chem. Phys. Discuss., 15, 26745–26793, 2015
www.atmos-chem-phys-discuss.net/15/26745/2015/
doi:10.5194/acpd-15-26745-2015

Atmospheric Chemistry and Physics Discussions

Understanding sources of organic aerosol during CalNex-2010 using the CMAQ-VBS

M. C. Woody[1], K. R. Baker[1], P. L. Hayes[2,3,4], J. L. Jimenez[3,4], B. Koo[5], and H. O. T. Pye[1]

[1]U.S. Environmental Protection Agency, Research Triangle Park, NC, USA
[2]Université de Montréal, Department of Chemistry, Montreal, QC, Canada
[3]Cooperative Institute for Research in Environmental Sciences (CIRES), University of Colorado, Boulder, CO, USA
[4]Department of Chemistry and Biochemistry, University of Colorado, Boulder, CO, USA
[5]ENVIRON International Corporation, Novato, CA, USA

Received: 23 July 2015 – Accepted: 12 September 2015 – Published: 5 October 2015

Correspondence to: H. O. T. Pye (pye.havala@epa.gov)

Published by Copernicus Publications on behalf of the European Geosciences Union.

Abstract

Community Multiscale Air Quality (CMAQ) model simulations utilizing the volatility basis set (VBS) treatment for organic aerosols (CMAQ-VBS) were evaluated against measurements collected at routine monitoring networks (Chemical Speciation Network (CSN) and Interagency Monitoring of Protected Visual Environments (IMPROVE)) and those collected during the 2010 California at the Nexus of Air Quality and Climate Change (CalNex) field campaign to examine important sources of organic aerosol (OA) in southern California.

CMAQ-VBS (OA lumped by volatility, semivolatile POA) underpredicted total organic carbon (OC) at CSN (−25.5 % Normalized Median Bias (NMdnB)) and IMPROVE (−63.9 % NMdnB) locations and total OC was underpredicted to a greater degree compared to the CMAQ-AE6 (9.9 and −55.7 % NMdnB, respectively; semi-explicit OA treatment, SOA lumped by parent hydrocarbon, nonvolatile POA). However, comparisons to aerosol mass spectrometer (AMS) measurements collected at Pasadena, CA indicated that CMAQ-VBS better represented the diurnal profile and the primary/secondary split of OA. CMAQ-VBS secondary organic aerosol (SOA) underpredicted the average measured AMS oxygenated organic aerosol (OOA, a surrogate of SOA) concentration by a factor of 5.2 (4.7 $\mu g\,m^{-3}$ measured vs. 0.9 $\mu g\,m^{-3}$ modeled), a considerable improvement to CMAQ-AE6 SOA predictions, which were approximately 24× lower than the average AMS OOA concentration. We use two new methods, based on species ratios and on a simplified SOA parameterization from the observations, to apportion the SOA underprediction for CMAQ-VBS to too slow photochemical oxidation (estimated as 1.5× lower than observed at Pasadena using $-\log(NO_x : NO_y)$), low intrinsic SOA formation efficiency (low by 1.6 to 2× for Pasadena), and too low emissions or too high dispersion for the Pasadena site (estimated to be 1.6 to 2.3× too low/high). The first and third factors will be similar for CMAQ-AE6, while the intrinsic SOA formation efficiency for that model is estimated to be too low by about 7×. For CMAQ-VBS, 90 % of the anthropogenic SOA mass formed was attributed to aged secondary semivolatile vapors

ACPD
15, 26745–26793, 2015

(70 % originating from volatile organic compounds (VOCs) and 20 % from intermediate volatility compounds (IVOCs)).

From source-apportioned model results, we found most of the CMAQ-VBS modeled POA at the Pasadena CalNex site was attributable to meat cooking emissions (48 %, and consistent with a substantial fraction of cooking OA in the observations), compared to 18 % from gasoline vehicle emissions, 13 % from biomass burning (in the form of residential wood combustion), and 8 % from diesel vehicle emissions. All "other" inventoried emission sources (e.g. industrial/point sources) comprised the final 13 %. The CMAQ-VBS semivolatile POA treatment underpredicted AMS hydrocarbon-like OA (HOA) + cooking-influenced OA (CIOA) at Pasadena by a factor of 1.8 (1.16 $\mu g\,m^{-3}$ modeled vs. 2.05 $\mu g\,m^{-3}$ observed) compared to a factor of 1.4 overprediction of POA in CMAQ-AE6, but did well to capture the AMS diurnal profile of HOA and CIOA, with the exception of the midday peak. We estimated that using the National Emission Inventory (NEI) POA emissions without scaling to represent SVOCs underestimates SVOCs by $\sim 1.7\times$.

1 Introduction

Organic matter is a ubiquitous component of $PM_{2.5}$. The Los Angeles South Coast Air Basin and San Joaquin Valley are designated as $PM_{2.5}$ nonattainment areas (http://www.epa.gov/oaqps001/greenbk/ancl.html), and major ground sites for the California at the Nexus of Air Quality and Climate Change (CalNex) campaign (Ryerson et al., 2013) were located within these basins at Pasadena and Bakersfield, respectively. Forty-one percent of the submicron aerosol mass at Pasadena was organic during CalNex (Hayes et al., 2013), and several complementary measurements of the organics including radiocarbon, secondary organic aerosol (SOA) tracers, OC/EC, organic aerosol (OA) composition, and volatile organic compounds (VOCs) (Zotter et al., 2014; Baker et al., 2015; Hayes et al., 2013) were collected.

ACPD
15, 26745–26793, 2015

Even in urban areas, SOA is expected to be comparable or dominate over primary organic aerosol (POA) (Zhang et al., 2007). Average O : C ratios exceed 0.3 in southern California (Craven et al., 2013), and over 70 % of midday OA is estimated to be secondary in Riverside, CA (Docherty et al., 2008), Mexico City (Aiken et al., 2009), and Pasadena, CA (Hersey et al., 2011; Hayes et al., 2013). Slightly more than half of the OC during CalNex was non-fossil in origin (Zotter et al., 2014; Baker et al., 2015). The dominant component of daytime SOA, semivolatile oxygenated organic aerosol (SV-OOA), at the Pasadena site was found to be highly correlated with measurements of fossil OC and markers of gasoline combustion indicating that fossil precursor gases are major contributors to its formation, consistent with an estimated 71 % fossil fraction (Zotter et al., 2014).

Several other studies have indicated that SOA from gasoline vehicles dominates over SOA from diesel vehicles as deduced from weekly cycles of non-fossil vs. fossil carbon and OA (Zotter et al., 2014; Bahreini et al., 2012; Hayes et al., 2013) as well as the higher potential for gasoline exhaust to form SOA in chamber oxidation experiments (Jathar et al., 2014). Borbon et al. (2013) further show gasoline vehicle emissions dominate the hydrocarbon distribution in urban areas such as CalNex, though measurements were limited to VOCs and excluded SVOCs and IVOCs. However, an alternative analysis using a detailed characterization of organic emissions from diesel and gasoline vehicles and estimated SOA yields concluded that diesel is responsible for more than 65 % of vehicle-attributable SOA (Gentner et al., 2012). In contrast, Ensberg et al. (2014) conclude that either the SOA yields in the atmosphere are much larger than have been observed in chambers, or alternatively vehicles may not be the dominant source of anthropogenic fossil SOA in Los Angeles. Recent work also indicates that models underestimate SOA from both known and unknown VOC precursors (Ensberg et al., 2014; Jathar et al., 2014; Zhang et al., 2014).

The Community Multiscale Air Quality (CMAQ) model (Byun and Schere, 2006) is used for research and regulatory purposes. POA is normally treated as nonvolatile (Simon and Bhave, 2012), and SOA forms mostly from gas-phase VOC oxidation to

ACPD
15, 26745–26793, 2015

form lower-volatility products with contributions from cloud processing (Carlton et al., 2010). Simulations using this traditional OA treatment in CMAQ (CMAQ-AE6) during CalNex (Baker et al., 2015) indicate that predicted OA is dominated by POA with a small contribution of SOA from aromatic and biogenic VOC oxidation in contrast to the SOA dominated picture from observations. While anthropogenic parent VOCs are well represented in the model, secondary organic carbon (SOC) from aromatics is underestimated (Baker et al., 2015). The model is likely missing sources of fossil carbon and tracer-based apportionment methods for SOC are unable to capture the total OA concentration. Hayes et al. (2015) indicates the SOA formed from the oxidation of VOCs alone is insufficient to explain observed SOA, and primary semi- and intermediate volatility compounds (S/IVOCs) are likely needed to explain the observed mass.

In this work, we examine the sources of OA in California with a focus on the 2010 CalNex-LA site in Pasadena, CA. In recognizing the potential role for S/IVOC emissions to form SOA (Robinson et al., 2007; Dzepina et al., 2009; Ahmadov et al., 2012), we employ the CMAQ-VBS model (Koo et al., 2014) and compare to the standard nonvolatile POA and SOA from VOCs in CMAQ v5.0.2. Our analysis focuses on the degree to which processes and/or sources characterized in CMAQ v5.0.2 may be responsible for OA observed as part of CalNex and the contribution of various sources to OA. We also identify whether underestimates in OA from CMAQ are due to emissions/dispersion, photochemical processing, or the OA treatment.

2 Methodology

The CMAQ model version 5.0.2 was applied to estimate air quality in California from 4 May to 30 June 2010, which coincides with the CalNex campaign (May and July 2010). Gas phase chemistry was simulated with the Carbon Bond 2005 (CB05) chemical mechanism (Yarwood et al., 2005). Aerosols were simulated using

ACPD
15, 26745–26793, 2015

the aerosols 6 (AE6) module with the volatility basis set (VBS) approach (Donahue et al., 2006) to model OA.

Details of the VBS treatment of organics in CMAQ are described in Koo et al. (2014). Briefly, CMAQ-VBS includes four distinct basis sets/OA groups: primary anthropogenic (corresponding to hydrocarbon-like OA (HOA)), secondary anthropogenic, secondary biogenic, and primary biomass burning. Each of the 4 basis sets is represented using 5 bins (4 bins to represent C^* values ranging from 10^0 to 10^3 $\mu g\,m^{-3}$ and 1 nonvolatile bin to represent C^* of 10^{-2} and 10^{-1} $\mu g\,m^{-3}$). Yields for semivolatile products of SOA from VOC precursors are the same as those used in Murphy and Pandis (2009) except for toluene (Hildebrandt et al., 2009). Yields for semivolatile products of SOA from IVOC precursors are based on the Murphy and Pandis (2009) reported yields for the SAPRC ARO2 model species, the model species that includes naphthalene (used in Pye and Seinfeld (2010) to represent IVOCs) (Koo et al., 2014). Photochemical reactions producing condensable vapors from aromatics (toluene, xylene, and benzene), isoprene, and monoterpenes utilize distinct high and low-NO_x yields (determined using $RO_2 + NO$ or $RO_2 + HO_2$; Chen and Griffin, 2005; Pfister et al., 2008; Carlton et al., 2010) while sesquiterpenes and IVOCs do not (IVOC NO_x-dependence excluded due to a lack of experimental data).

While experimental data suggests aging of both anthropogenic SOA (Hildebrandt et al., 2009) and biogenic SOA (Donahue et al., 2012) occurs, in CMAQ-VBS only anthropogenic SOA (formed from both VOCs and IVOCs) is aged via reactions of the gas-phase semivolatiles with OH using a rate constant of 2×10^{-11} $cm^3\,molec.^{-1}\,s^{-1}$ (twice the rate previously assumed for anthropogenic SOA aging (Murphy and Pandis, 2009) and based on results from the 2-D VBS; Donahue et al., 2013). Anthropogenic SOA aging reactions form products with a vapor pressure reduced by one order of magnitude (10×). Biogenic aging is turned off in CMAQ-VBS by default as previous results, using a more conservative aging scheme than in CMAQ-VBS, indicated VBS overpredicted OA in rural areas when biogenic SOA was aged (Lane et al., 2008; Murphy and Pandis, 2009; Fountoukis et al., 2011). In recognizing the aging of biogenic

ACPD
15, 26745–26793, 2015

SOA does occur, we perform a sensitivity simulation with biogenic aging on, the results of which are presented in Sect. 3.4.2. In excluding aging of biogenic SOA in all but our sensitivity simulation, we effectively assume that the net result of functionalization (aging) and fragmentation, which is more important for biogenic SOA than POA (Donahue et al., 2012), does not increase biogenic SOA concentrations (Fountoukis et al., 2011).

Primary SVOCs are aged in the gas-phase by reactions with OH using a rate constant of 4×10^{-11} cm^3 molec.$^{-1}$ s^{-1} (Robinson et al., 2007), lowering volatility by an order of magnitude and a portion (~ 10 %) of the OA mass shifted from the POA to the SOA set (Koo et al., 2014). This approach improves computational efficiency as it utilizes existing POA and SOA basis sets to represent oxidized POA and maintain the correct O : C ratios, avoiding the need for an additional oxidized POA basis set. With this treatment, the majority (~ 90 %) of slightly aged POA (after a single aging reaction) resides as POA-like while very aged POA (after four aging reactions) would reside as two-thirds POA and one-third SOA.

The model domain covered California and Nevada with a 4 km (317 × 236) grid resolution (Fig. 1). The vertical domain included 34 layers and extended to 50 mb. The first 11 days of the simulation were treated as a spin-up and results were excluded from the analysis to minimize the influence of initial conditions.

United States anthropogenic emissions were based on version 1 of the 2011 National Emissions Inventory (NEI) (US Environmental Protection Agency, 2014a). Stationary point sources reporting continuous emissions monitor (CEM) data were modeled with day and hour specific emissions matching the simulation period. Wildfire emissions were day specific although have little impact in Pasadena during this time period (Bahreini et al., 2012; Hayes et al., 2013). Biogenic emissions were day and hour specific using Weather Research Forecast (WRF) model temperature and solar radiation as input to the Biogenic Emission Inventory (BEIS) version 3.14 model (Carlton and Baker, 2011). Anthropogenic emissions from Mexico were projected to 2010 from 1999 (US Environmental Protection Agency, 2014b). All emissions were processed for

ACPD
15, 26745–26793, 2015

input to CMAQ using the Sparse Matrix Operator Kernel Emissions (SMOKE) modeling system (Houyoux et al., 2000).

Gridded meteorological variables used for input to CMAQ and SMOKE were generated using version 3.1 of the WRF model, Advanced Research WRF core (Skamarock and Klemp, 2008). Details regarding the WRF configuration and application are provided elsewhere (Baker et al., 2013). In general, surface meteorology and daytime mixing layer heights were well represented for this period in California. A 36 km CMAQ simulation covering the continental United States for the same time period was used to generate boundary conditions for this simulation. A global GEOS-CHEM (v8-03-02) (Bey et al., 2001) simulation provided boundary inflow for the 36 km continental scale CMAQ simulation (Henderson et al., 2014). Neither larger scale simulation included CMAQ-VBS OA species, though the impact is likely small as we assume most of the OA at Pasadena originates from local or regional sources located in our modeling domain.

POA is treated as semivolatile (SVOCs) in CMAQ-VBS and allowed to partition between the gas and particle phase. CMAQ-VBS also includes a formation pathway of SOA from the oxidation of IVOC emissions, which represents additional SOA precursor mass introduced into the model relative to CMAQ-AE6. CMAQ-VBS internally estimates SVOC and IVOC emissions at runtime based on traditional POA emission inventories. In the configuration used here, SVOC emissions are equivalent to the POA emissions input, i.e. no scaling of POA is applied to calculate SVOC emissions based on the assumption that the POA emission inventory is reported before evaporation of semivolatile emissions (Robinson et al., 2007). Therefore, the total mass of SVOC (gas and particle phase) emissions are equal to traditional POA emissions. IVOC emissions are estimated as 1.5 × SVOCs (Robinson et al., 2007), or 1.5× the traditional POA emission inventory. OH is artificially recycled (i.e. not depleted) in oxidation reactions of IVOCs and SVOCs (primary and secondary) to prevent double counting and impacts to the gas-phase chemistry of the underlying chemical mechanism. Although most modeling studies set IVOCs = 1.5 × SVOCs, the total amount of material introduced into the

ACPD
15, 26745–26793, 2015

model varies depending on the study and leads to varying importance of SOA from S/IVOCs and VOCS in different simulations. For example, in the box modeling studies of Dzepina et al. (2009) and Hayes et al. (2015) the POA was set equal to the measured HOA, then the SVOCs were calculated from equilibrium partitioning using the Robinson et al. (2007) volatility distribution, and then IVOC were set to 1.5 × SVOC. In grid-based model studies examining Mexico City OA (Hodzic et al., 2010; Tsimpidi et al., 2010; Shrivastava et al., 2011), the POA emission inventory was assumed to represent the fraction of aerosol remaining after evaporation of semivolatile emissions based on comparisons with observations and therefore SVOC emissions were set to 3 × traditional POA emissions and IVOC emissions were set to 1.5 × SVOC emissions leading to a total of S/IVOC = 7.5 traditional POA.

The volatility split of SVOC emissions in CMAQ-VBS is provided in Table 1. By default, CMAQ-VBS assigns volatility distributions for POA emissions from gasoline vehicles (GV), diesel vehicles (DV), biomass burning (BB), nonvolatile sources (NV), and "other" sources (OP) (e.g. point/industrial sources). In the absence of source specific POA emissions, the "other" profile is used. In our application, a significant portion of POA was associated with meat cooking activities (Table 2), which thermodenuder data suggests is of lower volatility compared to the other CMAQ-VBS source specific POA categories (Huffman et al., 2009). We roughly approximated a new volatility distribution for meat cooking SVOC emissions (Table 1) by altering the CMAQ-VBS biomass burning SVOC volatility distribution based on comparisons of meat cooking and the MILAGRO average biomass burning thermodenuder measured volatility (Huffman et al., 2009). This is meant as a first approximation and represents an area where further research is needed. We note thermodenuder data provides some constraints on SVOCs but no constraints on IVOCs, therefore the IVOC emissions from meat cooking remained unchanged (1.5× of meat cooking POA emissions).

After input into CMAQ-VBS, anthropogenic POA emission source specificity is lost as anthropogenic POA is lumped into a single basis set. In order to leverage our source specific emission inputs, in this study basis sets for POA from gasoline vehicles, diesel

ACPD
15, 26745–26793, 2015

vehicles, and meat cooking activities were added to provide anthropogenic POA source apportionment.

Ground-based CalNex measurements were collected in Pasadena, CA from 15 May to 15 June 2010 (Ryerson et al., 2013). The Pasadena sampling site was located on the California Institute of Technology campus, northeast of the Los Angeles metropolitan area and south of the San Gabriel Mountains. Both filter-based carbon measurements and Aerosol Mass Spectrometry (AMS) PM measurements were collected at this site. The filter-based measurements provide 23 h average concentrations of organic carbon, elemental carbon, and total carbon as well as the non-fossil vs. fossil carbon fraction. Additional details of the filter-based measurements, including comparisons of those measurements against traditional CMAQ (CMAQ-AE6) results, can be found in Baker et al. (2015). The AMS data provide real time (sub-hourly) measurements of speciated sub-micron PM, including various organic components as determined using positive matrix factorization (PMF). The AMS organic components resolved at the site include two types of SOA (semivolatile oxygenated OA (SV-OOA) consistent with fresher SOA mostly from urban areas, and low-volatility oxygenated OA (LV-OOA) consistent with aged SOA); two types of POA (hydrocarbon-like OA (HOA) and cooking-influenced OA (CIOA)); and local OA (LOA). The source of LOA, which accounts for approximately 5 % of OA mass at Pasadena, is generally unknown, though large fluctuations in measured concentrations suggest a local source (Hayes et al., 2013). Additional details regarding the AMS measurements and PMF component analysis can be found in Hayes et al. (2013).

3 Results and discussion

3.1 Comparison against routine monitoring networks

Average OA concentrations predicted by CMAQ-VBS during 15 May to 30 June were highest in the Greater Los Angeles Area where the domain maximum concentration

ACPD
15, 26745–26793, 2015

was 3.1 $\mu g\,m^{-3}$ (Fig. 1). In this region, OA was approximately 30–50 % of total modeled $PM_{2.5}$ and modeled OA was generally evenly split between primary and secondary (i.e. SOA comprised 40–60 % of OA). In contrast, CMAQ-AE6 predicted the majority (80–90 %) of OA was comprised of POA in LA. The shift from primary dominated to a more even primary/secondary split in CMAQ-VBS is due to both the semivolatile treatment of POA (lowering POA concentrations) and additional SOA formation pathways (SOA from IVOCs and SOA aging as discussed in Sect. 3.4.2).

Model performance comparisons at IMPROVE and CSN sites in California and Nevada indicated CMAQ-VBS generally underpredicted OC (Table 3). Model performance for OC was slightly degraded (i.e. greater underprediction) compared to CMAQ-AE6 predictions (see Table S3 and Fig. S9 of the Supplement for CMAQ-AE6 model performance). While CMAQ-VBS predicted higher concentrations of SOA due to additional SOA formation pathways (see Table S2 in the Supplement), including the introduction of IVOCs mass into the modeling system, the additional SOA production did not compensate enough for the evaporated POA or improve performance relative to routine network measurements.

The degraded OC model performance (with the exception of slightly improved error) was more evident at CSN sites, which are often located closer to anthropogenic emission sources. At those sites, CMAQ-AE6 OC normalized median bias (NMdnB) and error (NMdnE) were 9.9 and 43.9 % compared to −25.5 and 36.5 % in CMAQ-VBS. At IMPROVE sites, CMAQ-AE6 NMdnB and NMdnE (−55.7 and 57.6 %) were comparable to CMAQ-VBS values (−63.9 and 64.6 %), with the negative bias indicating both consistently underpredicted OC.

CMAQ-VBS also underpredicted OC compared to filter-based and AMS measurements at the Pasadena CalNex site, which were in reasonably good agreement with one another (Fig. 2). CMAQ-VBS OC predictions were approximately 2 to 3× lower than measured OC, with the largest gaps generally occurring during photochemically active periods (e.g. 4 to 7 June) when OOA concentrations were higher (Fig. 3), suggesting the model underpredicts SOA.

ACPD
15, 26745–26793, 2015

3.2 Comparison against CalNex measurements at Pasadena

Figures 3 and 4 compare CMAQ-VBS results against AMS measured submicron OA PMF components, where CMAQ-VBS POA from meat cooking sources was compared against AMS CIOA, CMAQ-VBS POA from all other sources including motor vehicles was compared against AMS HOA, and CMAQ-VBS SOA was compared against AMS SV-OOA + LV-OOA. Additional AMS measurements of LOA and CMAQ-VBS biomass burning OA (BBOA) are included in Fig. 4 but these measurements/model results do not have a direct corresponding AMS/model value.

3.2.1 Meat cooking OA

CMAQ-VBS CIOA concentrations averaged 0.65 $\mu g\,m^{-3}$ (28 % of modeled OA) at Pasadena during the modeling period with a diurnal profile that was generally flat throughout the day and peaked at night. This is compared to an average AMS CIOA concentration of 1.22 $\mu g\,m^{-3}$ (17 % of measured OA) and a diurnal profile that peaked in the afternoon and at night, with peaks occurring slightly later than typical mealtimes and likely due to transport time (Hayes et al., 2013). The AMS diurnal profile is consistent with AMS measurements from several major urban areas, including Barcelona, Beijing, London, Manchester, New York City, and Paris (Allan et al., 2010; Huang et al., 2010; Sun et al., 2011; Mohr et al., 2012; Freutel et al., 2013). CMAQ-VBS generally compared well to AMS measurements in the morning but underpredicted the afternoon peak by 3.8× and evening peak by 2.8×.

We examined the theoretical partitioning of modeled CIOA using AMS measured OA (in place of modeled OA) to determine if partitioning alone explained the low bias in modeled midday CIOA concentrations. This scenario only increased modeled CIOA by approximately 10 % in the afternoon. If instead the modeled CIOA was treated as nonvolatile (100 % of emissions located in the particle phase), model concentrations increased by 30–40 % and generally improved model performance (−32 % normalized median bias compared to −51 % in the semivolatile treatment). However, the modeled

ACPD
15, 26745–26793, 2015

CIOA would still underpredict the afternoon and evening peaks by 2.9× and 2×, respectively.

Even a nonvolatile treatment was unable to reproduce the measured peaks, suggesting the model CIOA emissions were low, particularly during afternoon and evening hours. This is expected since the emission inventory excludes residential meat cooking due to uncertainty in emission fraction and activity data and the inclusion of these emissions would ameliorate some of the underprediction bias in evening hours and on weekends. To account for missing residential meat cooking emissions and potential underestimates in commercial meat cooking emissions, a doubling of CIOA emissions did well to reproduce the averaged measured value (1.28 $\mu g\,m^{-3}$ modeled vs. 1.22 $\mu g\,m^{-3}$ measured). However, the diurnal profile applied in SMOKE to the majority of CIOA emissions (profile 26) is a low arcing profile that peaks at 15:00 LST (see Fig. S14 in the Supplement). Additional mass of emissions applied to this profile helped to capture average CIOA and improved underpredictions of the evening peak (lowered from 2.8× to 1.3×) but overpredicted measurements in the morning and maintained the underprediction of afternoon AMS-measured CIOA (Fig. S13), suggesting some morning emissions should be reallocated to occur in the afternoon. It is also possible that some of the measured CIOA peak was due to photochemistry, as the afternoon peak coincides with the peak in AMS SV-OOA. Given the evening peak in measured CIOA occurs during a period of relatively low photochemistry (21:00 LST), it would seem emissions are a more plausible cause for the underprediction. Furthermore, trends in hourly data supports the theory that CIOA was more influenced by emissions than photochemistry, as CIOA concentrations do not increase as sharply as AMS SV-OOA during photochemically active periods (e.g. 4 to 7 June) (Fig. 3) and the afternoon peak corresponds to the arrival of the morning emissions from downtown LA to the Pasadena site.

The highest observed CIOA value (8.9 $\mu g\,m^{-3}$) occurred on 30 May at 20:00 LST, which corresponds to the Saturday of the Memorial Day Holiday weekend. Results from Zotter et al. (2014), who reported a high non-fossil fraction of OA at the CalNex site

ACPD
15, 26745–26793, 2015

on 30 May, corroborate the AMS data. SMOKE/CMAQ emission processing does not allocate more emissions to holidays like Memorial Day for meat cooking, when a larger number of people grill meat and emissions are likely to be higher than normal. Therefore, we would not expect CMAQ to reproduce such events. When the CIOA measurements during the Memorial Day weekend were excluded, the midday and evening AMS peaks were reduced by 0.2 $\mu g\,m^{-3}$ and 0.5 $\mu g\,m^{-3}$, respectively, which corresponds to CMAQ-VBS underpredictions of 3.3× and 2.2× (or 2.5× and 1.6× for nonvolatile emissions and 1.4× and 1× for a doubling of CIOA emissions).

Given that the majority of both modeled and measured POA at Pasadena was attributable to cooking sources, further evaluation of the total CIOA emissions as well as the diurnal profile and volatility distribution applied to those emissions may help to improve POA model performance in urban areas.

3.2.2 Other POA

Generally, CMAQ-VBS POA results (excluding meat cooking) compared reasonably well against AMS HOA measurements (Fig. 4) in total magnitude, particularly during morning and evening hours. However, modeled POA was biased low, more so in the afternoon. The modeled POA underpredicted the AMS HOA peak (which occurred at 14:00 LST) by a factor of 3 compared to underpredictions of 7–55 % (average of 31 %) during morning (00:00–10:00 LST) and evening (19:00–23:00 LST) hours. The modeled POA peak instead occurred at night (likely due to the collapse of the planetary boundary layer) which did correspond to a measured evening peak offset by ~ 1 h.

We estimated that when underpredictions in modeled total OA were accounted for, partitioning to the particle phase increased POA concentrations by 20 % and the afternoon underprediction of POA was reduced to 2.3×, though performance in the morning and evening remained relatively unchanged. When POA was instead treated as nonvolatile (CMAQ-AE6, where CMAQ-AE6 POA = CMAQ-VBS SVOC = NEI POA), the model overpredicted AMS measurements in the morning and evening (by 1.5 to 1.8×) and underpredicted measurements in the afternoon (by 1.5 to 1.6×). The resulting

ACPD
15, 26745–26793, 2015

diurnal pattern (Fig. S12, higher in the morning and evening, with a minimum in the afternoon) was opposite the AMS measurements (lower in the morning and evening, peaked in the afternoon).

While neither POA volatility treatment captured the afternoon peak in measured POA, the semivolatile treatment predictions during morning and evening hours suggest it to be the more appropriate model representation of the two. However, further considerations are needed to better account for the AMS measured midday peak in POA. The measured HOA peak followed a similar pattern to OOA both in the diurnal profile (Fig. 4) and on an hourly basis (Fig. 3), which may suggest that photochemistry served a role in the measured HOA peak as additional OA mass attributed to photochemistry could promote partitioning of semivolatile HOA to the particle phase. However, photochemical age and CO are correlated at this location due to the arrival of downtown LA plume in the early afternoon, so the observed correlation should not be over-interpreted. Alternative aging schemes to the Robinson et al. (2007) approach used in CMAQ-VBS, such as those proposed by Grieshop et al. (2009) and Pye and Seinfeld (2010) generally produce more OA mass than the Robinson et al. (2007) scheme and could better represent the POA midday peak (Hayes et al., 2015). These alternative aging schemes may also degrade the morning and evening performance, though Hayes et al. (2015) found the Grieshop et al. (2009) scheme performed reasonably well throughout the day.

Average CMAQ-VBS POA concentrations were approximately a factor of 1.6 lower than AMS measured HOA values at Pasadena (0.51 vs. 0.83 $\mu g\,m^{-3}$). Increasing the CMAQ-VBS POA emissions by a factor of 1.5 produced average modeled POA concentrations (0.78 $\mu g\,m^{-3}$) comparable to the AMS-measured HOA, though the model overpredicted HOA in the morning and evening and underpredicted HOA in the afternoon (Fig. S15). These results suggest the NEI underestimates non-cooking related SVOCs by $\sim 1.5\times$ and cooking related SVOCs by $\sim 2\times$ and our SVOCs emissions are approximately 1.5 to $2\times$ lower than those estimated using measured HOA at Pasadena in Hayes et al. (2015).

ACPD
15, 26745–26793, 2015

A source of uncertainty in the POA results is the volatility distribution used for industrial/point sources (i.e. "other" sources) is based on measurements made from diesel generator exhaust (Robinson et al., 2007). However, we assume this has less impact than missing emissions since the nonvolatile POA treatment underpredicted the measurements and POA from these sources only comprises 13 % of total modeled POA, or 25 % excluding CIOA (Sect. 3.4.1).

3.2.3 SOA

Similar to the routine measurement comparisons of total OC, CMAQ-VBS underpredicted AMS OOA (SV-OOA + LV-OOA). This is consistent with many regional air quality models (Volkamer et al., 2006; De Gouw et al., 2008), including CMAQ (Foley et al., 2010), which often underpredict urban SOA. Other regional models that use high S/IVOC emissions to approximately match the observed POA do match or even exceed the urban observations (e.g. Hodzic et al., 2010; Shrivastava et al., 2011) though we found this not to be the case in CMAQ-VBS. The diurnal pattern of CMAQ-VBS SOA is generally more consistent with measurements of SV-OOA compared to LV-OOA (Fig. S8). The fact that LV-OOA is heavily oxidized and has relatively constant concentrations suggest it to be a background source, comprised of OA formed elsewhere and transported to Pasadena (Hayes et al., 2015). Note, the diurnal profile of CMAQ-AE6 SOA (Fig. S9) formed from particle oligomerization (a process not included in CMAQ-VBS) did follow a similar pattern to AMS LV-OOA (relatively flat throughout the day with a midday/afternoon bimodal peak) but model concentrations were significantly (~ 40×) lower (Fig. S10).

CMAQ-VBS predicted considerably more SOA mass than CMAQ-AE6 (~ 0.9 $\mu g\,m^{-3}$ at Pasadena in CMAQ-VBS compared to ~ 0.2 $\mu g\,m^{-3}$ for CMAQ-AE6). Overall, CMAQ-VBS SOA diurnal concentrations were approximately 4 to 5.4× lower than the AMS OOA, with the largest underestimate corresponding to the peak AMS measurement (13:00 LST). The underprediction could be attributed to low emissions, low photo-

ACPD
15, 26745–26793, 2015

chemical age, too much dispersion or too little transport of emissions to the Pasadena site in the model, or low intrinsic SOA production efficiency.

Comparisons of modeled and measured CO normalized for background CO (ΔCO, where $\Delta CO = CO - CO_{background}$ and modeled $CO_{background} = 75$ ppb, see Hayes et al. (2013) for CO background measurements) show 300 ppb measured ΔCO vs. 150 ppb modeled ΔCO. This observation suggests CMAQ anthropogenic CO emissions, which are often used as a proxy for anthropogenic emissions, may be a factor of two too low, or alternatively that too high dispersion and/or too low transport of emissions to Pasadena in the model results in the lower modeled CO. Baker et al. (2015), who also used the 2011 NEI, reported a similar model underprediction (approximately a factor of two) for total VOCs at Pasadena. However, Baker et al. (2015) reported the 2011 NEI based SOA precursor concentrations were in relatively good agreement with measured values, though xylene and toluene were generally overpredicted which could be attributed to underpredictions in photochemical age leading to insufficient xylene oxidation (e.g. at 0.1 day photochemical age, ∼ 75 % of emitted xylene would remain, but at actual ambient photochemical age a larger fraction would have reacted). CMAQ SOA precursor concentrations were a factor of 1.2 too low compared to 3 h measurements and a factor of 1.1 too high compared to 1 h measurements, suggesting the SOA precursor to CO emission ratio was incorrect by a factor of 2. Comparisons of the ratio of xylene and toluene emissions to CO emissions in LA and Orange Counties against observed xylene and toluene extrapolated to zero photochemical age (to account for photochemistry) to observed CO support this, as the emissions ratio (0.030) is approximately twice the observed ratio (0.014).

The role of photochemical age in SOA underpredictions was explored at Pasadena by examining SOA formed (plotted as SOA/ΔCO to approximately correct for differences in emissions and dilution between times) in CMAQ-VBS vs. photochemical age (estimated using $-\log(NO_x/NO_y)$; Kleinman et al., 2008) (Fig. 5). The slope of the best fit line ($66\,\mu g\,m^{-3}\,ppm^{-1}$) was low by ∼ 1.6 × compared to the measured value of $108\,\mu g\,m^{-3}\,ppm^{-1}$ (Hayes et al., 2015). However, when the lower ΔCO in CMAQ

ACPD
15, 26745–26793, 2015

is accounted for, the best estimate for the underprediction is 3.2×. Compared to the measured photochemical age (estimated by $-\log(NO_x/NO_y)$), the photochemical age component of CMAQ-VBS SOA was low by ~ 1.5×, which helps explain part of the underprediction in SOA concentrations (Figs. 3 and 4) but not on SOA production efficiency (Fig. 5). For reference, Fig. 5 also includes the slope for CMAQ-AE6 predictions ($8\,\mu g\,m^{-3}\,ppm^{-1}$), which was much lower than the slope for CMAQ-VBS and also much lower than observations for multiple urban areas (De Gouw and Jimenez, 2009).

Examining modeled SOA vs. odd oxygen ($O_x \equiv O_3 + NO_2$) (Herndon et al., 2008; Wood et al., 2010), which leverages high measured correlations of SOA and O_x with generally good model performance of O_x (true for Pasadena during CalNex; Kelly et al., 2014), the slope for CMAQ-VBS was $72\,\mu g\,m^{-3}\,ppb\,V^{-1}$ (Fig. 5). This is approximately a factor of 2 lower than observations at Pasadena ($146\,\mu g\,m^{-3}\,ppb\,V^{-1}$) (Hayes et al., 2013), where measurements were comparable to other urban areas (Wood et al., 2010; Morino et al., 2014; Zhang et al., 2015). In comparison, CMAQ-AE6 (which has identical O_x concentrations to CMAQ-VBS) underpredicted the metric by a factor of 16, again suggesting that while CMAQ-VBS underpredicts SOA, it does considerably better than the traditional CMAQ-AE6 SOA treatment. Note, in CMAQ-VBS sensitivity simulations without aging reactions (Sect. 3.4.2) the slope of SOA vs. O_x ($11\,\mu g\,m^{-3}\,ppb\,V^{-1}$) was nearly equivalent to the slope of CMAQ-AE6 ($9\,\mu g\,m^{-3}\,ppb\,V^{-1}$). This indicates most of the CMAQ-VBS SOA mass was produced as a result of aging of SVOCs and is further discussed in Sect. 3.4.2.

Thus our analysis suggests that the SOA production efficiency in CMAQ-VBS is too low by 1.6 to 2×; photochemical age low by a factor of 1.5×, and the remaining underprediction (1.6 to 2.3×) attributed to other factors (emissions, transport, etc.). Combining both underestimates of the SOA/ΔCO (1.5× and 3.2×) implies that SOA concentrations should be too low by 4.8×, which agrees with the 5.2× underprediction of SOA compared to AMS OOA.

One possible reason for the underestimate of SOA production efficiency in CMAQ-VBS (and CMAQ-AE6) is that CMAQ SOA yields do not account for SVOC wall loss,

ACPD
15, 26745–26793, 2015

which Zhang et al. (2014) indicated reduce SOA production by 2 to 4×. However, the factor of 4 is for alkane systems (speciated long alkanes are not considered SOA precursors in CB05) and toluene and specific to the smog chamber used in Zhang et al. (2014). Therefore, SVOC wall loss does not likely account for the entire underestimate of SOA production efficiency.

Another possibility for the underprediction of SOA in CMAQ-VBS is SOA formed from missing or mischaracterized (as unspeciated VOCs) IVOC emissions. There is significant uncertainty currently associated with IVOC emissions and their SOA yields. Current CMAQ-VBS IVOC emissions are scaled to primary SVOC emissions (1.5×) based on the results of a diesel generator (Robinson et al., 2007). Jathar et al. (2014) recently published updated IVOC emission factors for unspeciated compounds and SOA yield parameterizations for diesel vehicles, gasoline vehicles, and biomass burning based on more recent source specific smog chamber results. Using the results of Jathar et al. (2014) to update the IVOC emissions and parameterization in CMAQ-VBS could help to bridge the gap between model and measurements, but likely would not account for the entire missing SOA mass as CMAQ-VBS simulations where S/IVOC emissions were increased by 3.75 × (SVOC = 1.5 × POA to match HOA, IVOC = 1.5 × SVOC), 5 × (SVOC = 2 × POA to match CIOA, IVOC = 1.5 × SVOC) and 7.5 × (SVOC = 3 × POA, IVOC = 1.5 × SVOC) continued to underpredict both average (by factors of 4.4×, 3.7×, and 2.9×) and daily peak (by factors of 4.6×, 3,9×, and 2.8×) measured OOA. When the factor of 7.5× is used, the model is in approximate agreement with the observations once the lower model photochemical age and low emissions/high dispersion are taken into account, which is consistent with previous modeling efforts for CalNex and elsewhere (Dzepina et al., 2009; Hodzic and Jimenez, 2011; Hayes et al., 2015). However, the approximate quantitative agreement may be for the wrong reasons and should not be over-interpreted as direct evidence of the presence and SOA formation efficiency of S/IVOCs.

ACPD
15, 26745–26793, 2015

3.3 Non-fossil vs. fossil carbon

In addition to tracking POA from meat cooking activities separately in CMAQ-VBS, we also added the ability to track POA from gasoline vehicles, diesel vehicles, and "other" sources separately. Tracking POA from various sources provided the opportunity to compare CMAQ-VBS non-fossil vs. fossil carbon contributions against filter-based measurements collected at Pasadena (Fig. 6) (Baker et al., 2015). Measurements indicated, on average, a near even split of non-fossil (48 %) and fossil (52 %) carbonaceous mass (Baker et al., 2015), and the non-fossil measurements were consistent with other collocated ^{14}C measurements collected during the same time period (51 % non-fossil) (Zotter et al., 2014).

On 6 days the measured non-fossil fraction was > 1 and therefore measurements on these days were excluded from our analysis as outliers. We believe these outliers were due to a plume from a nearby medical waste incinerator passing directly by the measurement site. Other results were likely also influenced by the incinerator, though to a lesser extent, biasing the non-fossil carbon fraction high.

For the purposes of the comparison, we assumed non-fossil carbon was comprised of biogenic SOC, biomass burning POC, and all meat cooking POC (measurements suggest ~ 75 % of meat cooking carbon is non-fossil but are likely biased due to imperfections of the PMF analysis; Hayes et al., 2013; Zotter et al., 2014). We assumed fossil carbon was comprised of EC, anthropogenic SOC, POC from gasoline and diesel vehicles, and all POC from "other" emission sources. Non-fossil carbon was always underpredicted in CMAQ-VBS (average predictions of 0.61 $\mu g\,C\,m^{-3}$ vs. average observation of 1.86 $\mu g\,C\,m^{-3}$) and the model predicted it to be dominated by meat cooking emissions. This suggests missing SOA formation pathways, low model SOA yields, or missing emission sources of non-fossil carbon at or upwind of Pasadena, including the substantial likely underestimate of cooking POA discussed above. Higher SOA formation from cooking emissions than parameterized here (Hayes et al., 2015) could account for some of the discrepancy, although this source is poorly characterized. In-

ACPD
15, 26745–26793, 2015

basin biogenic SOA (e.g. formed from VOCs emitted within the LA basin) and advection of marine OA are estimated to be very small (Hayes et al., 2015), and are unlikely to account for the noted discrepancy. Not enough formation and/or advection of biogenic SOA from the North may account for some of the missing non-fossil SOA as well (Hayes et al., 2015).

Contrastingly, CMAQ-VBS did a reasonably good job of predicting fossil carbon at Pasadena (average predictions of 1.81 $\mu g\,C\,m^{-3}$ vs. average observation of 1.97 $\mu g\,C\,m^{-3}$), though the model tended to underpredict fossil carbon during days with higher measured OOA (e.g. 4 to 10 June, Fig. 3). Fossil carbon was generally dominated by EC and anthropogenic secondary organic carbon (ASOC). Comparisons of CMAQ-VBS EC (which has an identical treatment in CMAQ-AE6) concentrations (average of 1.01 $\mu g\,C\,m^{-3}$) against CalNex filter-based measurements at Pasadena (0.51 $\mu g\,C\,m^{-3}$) suggest that CMAQ-VBS (and CMAQ-AE6) overpredicted EC and therefore over emphasizes its contribution to total carbon. Excluding EC, CMAQ-VBS predicted considerably less non-EC fossil carbon (average of 0.80 $\mu g\,C\,m^{-3}$) compared to observed (1.46 $\mu g\,C\,m^{-3}$) (Fig. S17). Additional details regarding the filter-based measurements and the EC / OC split in the NEI are reported in Baker et al. (2015).

Comparisons of the CMAQ-VBS diurnal profiles for non-fossil and fossil carbon at Pasadena against measurements made by Zotter et al. (2014) indicated the model did well to capture the overall pattern of the measurements (higher non-fossil carbon in the morning and evening with the minimum occurring in the afternoon) but was biased towards fossil carbon (see Fig. S18 of the Supplement). The fact that the model represented the measured diurnal pattern well but was biased suggests that it was missing both non-fossil (in the morning and evening) and fossil sources (in the afternoon). This is consistent with model underpredictions of meat cooking POA (non-fossil) in the morning/evening, minimal contributions from model SOA (non-fossil) throughout the day, and underpredictions of the afternoon peak in anthropogenic SOA (fossil).

ACPD
15, 26745–26793, 2015

3.4 CMAQ-VBS sensitivity analysis

3.4.1 POA source apportionment

Higher CMAQ-VBS predictions of POA from gasoline vehicles compared to diesel vehicles was true throughout southern California (Fig. 7). Most POA was comprised of meat cooking POA, followed by POA from gasoline vehicles, "other" sources, and finally diesel vehicles. Note that the diesel vehicle panel in Fig. 7 required a scale an order of magnitude lower than the other sources. At Pasadena, the breakdown of POA was as follows: 48 % meat cooking, 18 % gasoline vehicles, 13 % biomass burning (in the form of residential wood combustion), 13 % "other", and 8 % diesel vehicles. This further emphasizes the relative importance of meat cooking activities relative to mobile sources as well as gasoline vehicle emissions compared to diesel vehicle emissions. We note that the predicted urban POA has larger non-fossil than fossil fraction.

Of note was the limited contributions of gasoline and diesel vehicle POC emissions to total carbon at Pasadena, where fossil OC was dominated by ASOC (Fig. 6). This result, coupled with the fact that the majority of ASOC precursor emissions originated from gasoline vehicles and point sources, suggest that gasoline vehicles dominated mobile source OC contributions (Bahreini et al., 2012; Gentner et al., 2012; Ensberg et al., 2014; Hayes et al., 2015).

3.4.2 Contributions from CMAQ-VBS SOA formation pathways

As a sensitivity study, the aging of secondary biogenic SVOCs was turned on using the same oxidation pathways used for the aging of secondary anthropogenic SVOCs in CMAQ-VBS. That is, secondary biogenic SVOCs were aged by reactions with OH in the gas-phase using a rate constant of 2×10^{-11} cm^3 molec.$^{-1}$ s^{-1} and each aging step reduced the volatility by an order of magnitude. The aging of biogenics produced more SOA at Pasadena ($\sim 0.5\,\mu g\,m^{-3}$ throughout the day) (Fig. 8). The diurnal profile indicates aged biogenic SOA concentrations were essentially constant throughout the

ACPD
15, 26745–26793, 2015

day, which is the same pattern as AMS LV-OOA. A scenario where LA basin biogenic SOA precursor emissions were zeroed out indicated almost all (95 %) of the predicted biogenic SOA originated from outside the basin, which is consistent with Hayes et al. (2015).

The additional non-fossil carbon mass from biogenic SOA would help to close the gap in the modeled vs. measured non-fossil carbon at Pasadena. Furthermore, the additional SOA mass improved overall OC model performance at routine monitoring network sites (Table 4) comparable to, if not better, than CMAQ-AE6 model performance. Monoterpene emissions were underestimated at Pasadena (Baker et al., 2015), although biogenic VOCs emitted in the LA basin make a very small contribution to SOA in Pasadena. Rather biogenic emitted in the Central Valley and surrounding mountains are thought to contribute most of the biogenic SOA observed in the basin (Hayes et al., 2015). CMAQ-VBS could potentially overestimate biogenic SOA if the underprediction of monoterpenes applies to other areas of California. Further evaluation of the impacts of biogenic SOA aging are needed, particularly in areas dominated by biogenic SOA, such as in the southeastern US.

Figure 8 also provides the contribution for the three standard SOA formation pathways in CMAQ-VBS (VOCs, IVOCs, and aging) at Pasadena. These were estimated using sensitivity simulations without IVOCs, aging, or both and then taking the difference between results from the various scenarios. The results indicate the majority of SOA was formed from aging, representing a technique to increase model SOA yields similar to the 4× increase in SOA yields proposed by Zhang et al. (2014) and used with CMAQ-AE6 in Baker et al. (2015). Additionally, CMAQ-VBS predicted comparable SOA (considering first generation only) from VOCs to CMAQ-AE6, which one would expect given that they utilize comparable SOA yields (see the Supplement for SOA yield curves). However, the inclusion of higher volatility semivolatile products (C^* of 100 and 1000) provides high yielding points along the yield curve missing in Odum 2-product framework of CMAQ-AE6. Thus, CMAQ-VBS transfers more mass from VOC precursor

ACPD
15, 26745–26793, 2015

to semivolatile oxidation product but requires the aging process to lower the volatility of the semivolatile product to the point of condensing to form SOA.

3.4.3 Simplified SOA parameterization

A simplified SOA parameterization (SIMPLE) has been presented (Hodzic and Jimenez, 2011; Hayes et al., 2015) and applied here in CMAQ to provide an alternative SOA modeling budget for comparison with AE6 and VBS. SIMPLE was originally developed by Hodzic and Jimenez (2011) and recently shown to perform well in predicting anthropogenic SOA at Pasadena (Hayes et al., 2015). A key goal of the parameterization is to provide a quick way to estimate the amount of anthropogenic SOA formed from pollution sources, especially for studies in which mechanistic SOA formation description is not the goal, but when having the correct amount of aerosol present is important for the results of the simulation. It can also serve as a simple-to-implement benchmark to compare more complex parameterizations across different models, when many other parameters are also changing. The parameterization uses a single SOA precursor (VOC^*) scaled to CO emissions and which reacts with OH. The oxidation product is treated as nonvolatile. However, it will likely need to be re-fitted to ambient data in the future, when emission control strategies change the ratio of VOC precursors to CO, or their average SOA yield.

Hayes et al. (2015) found that the SIMPLE parameterization compared favorably to measurements and VBS box model results at Pasadena. In our implementation in CMAQ-VBS, we use an emission rate of $0.069\,\mathrm{g\,VOC^*\,g^{-1}\,CO}$ and a $k_{OH} = 1.25 \times 10^{-11}\,\mathrm{cm^3\,molec^{-1}\,s^{-1}}$, based on the optimum values for Pasadena reported in Hayes et al. (2015).

SIMPLE predicted more anthropogenic SOA mass than CMAQ-VBS (2.5× more at the afternoon peak) (Fig. 9) with the right diurnal cycle. However, it still underpredicted the AMS measured SV-OOA by a factor of 2.3× at the afternoon peak. The slope of SOA/ΔCO vs. $-\log(NO_x/NO_y)$ for SIMPLE was $113\,\mu\mathrm{g\,m^{-3}\,ppm^{-1}}$, which was slightly

ACPD
15, 26745–26793, 2015

more than the measured 108 $\mu g\,m^{-3}\,ppm^{-1}$ and suggests that the SIMPLE parameterization is performing as expected and has an intrinsic SOA formation efficiency consistent with the observations. Underpredictions of photochemical age and low emissions/too high dispersion most likely explain the observed difference, as CO was underpredicted both in this study (see the Supplement) and in Baker et al. (2015). The factor of 2 difference in modeled vs. measured CO indicated in Sect. 3.2.3 are similar to the 2.3× underprediction in SIMPLE. This shows that the use of SIMPLE in a model can help diagnose model problems that are unrelated to the model intrinsic SOA formation efficiency. CO inventories can also be estimated from ambient data (e.g. Brioude et al., 2013), providing an alternative if the quality of official inventories degrades in the future.

4 Conclusions

The application of the CMAQ-VBS over California and Nevada in May and June 2010 was found to underpredict OC at routine monitoring networks, likely due to underpredictions of SOA (missing formation pathways, emissions, formation efficiency, etc.). The underprediction of CMAQ-VBS was more pronounced than CMAQ-AE6, particularly at CSN monitors (Table 3 and Table S3) which are primarily located in urban areas and where modeled POA comprised a higher percentage of OC, and therefore likely attributed to the semivolatile treatment of POA in CMAQ-VBS. However, the lower CMAQ-VBS POA appears to correct for a compensating bias of CMAQ-AE6 POA overpredictions as CMAQ-VBS was able to better capture the POA/SOA split, total POA mass, and total SOA mass compared to AMS measurements at Pasadena. CMAQ-VBS predicted less POA (as a result of evaporation) and more SOA (90 % attributed to aging of anthropogenic SOA) compared to CMAQ-AE6.

CMAQ-VBS underpredicted the measured AMS OOA midday peak by 5.4×, albeit to a lesser extent than CMAQ-AE6 predictions (38×). Using two new methods, one based on species ratios and the other based on a simplified SOA parameterization from the

ACPD
15, 26745–26793, 2015

observations, we apportioned the SOA underprediction from CMAQ-VBS to too slow photochemical oxidation based on $NO_x : NO_y$ (1.5× lower than observed at Pasadena), too low intrinsic SOA efficiency (1.6 to 2× too low for Pasadena), and too low emissions/high dispersion for the Pasadena site (1.6 to 2.3× too low/high). Individually, none of the recently proposed updates for SOA predictions (SVOC wall loss (Zhang et al., 2014), unspeciated IVOCs (Jathar et al., 2014), aging of biogenic SOA (Donahue et al., 2012), and aging of SVOCs/IVOCs) can resolve the model/measurement discrepancy, but a combination of the factors may.

POA at the Pasadena CalNex site was found to be mostly from meat cooking emissions (48 %) and to lesser extents from gasoline vehicle emissions (18 %), diesel vehicle emissions (8 %), biomass burning (13 %), and "other" emissions (13 %), and interestingly more than 50 % non-fossil. Furthermore, the semivolatile treatment of POA better represented the measured AMS diurnal profile of HOA than nonvolatile POA, particularly during morning and evening hours. Using sensitivity simulations, we estimated the NEI POA captures approximately 50 % of meat cooking SVOCs and approximately 66 % from all other sources. However, CMAQ-VBS underpredictions of POA may also be attributed to the volatility distribution applied to emissions or missing/mischaracterized POA oxidation and increasing CMAQ-VBS emissions by 1.5 to 2× would degrade POA model performance in the morning and evening.

Regarding which OA treatment is more appropriate, CMAQ-VBS or CMAQ-AE6, depends on the user's modeling needs and goals. The traditional treatment more accurately predicts total OA measured at routine monitoring networks (though due to possible compensating model biases, particularly at sites located in urban areas which are more influenced by POA). Conversely, CMAQ-VBS better represents the total SOA mass and the POA/SOA split at Pasadena. Due to the difference in SOA/POA splits, the two CMAQ configurations may respond differently to VOC and/or NO_x emission reductions, which should be examined in future work.

A future extension of this work includes enhancements to SOA from IVOCs in CMAQ. IVOC emissions are currently scaled to POA. Recent results published by Jathar et al.

ACPD
15, 26745–26793, 2015

(2014) provide new insights in how to better estimate IVOC emissions from gasoline and diesel vehicles and biomass burning. With updated IVOC emissions and parameterizations, coupled with comparisons of IVOC measurements made during CalNex (Zhao et al., 2014), CMAQ-VBS predictions may be able to close the gap between measured and modeled SOA and provide additional certainty in both IVOCs and the SOA formed from IVOCs.

The Supplement related to this article is available online at doi:10.5194/acpd-15-26745-2015-supplement.

Acknowledgements. The authors would like to acknowledge John Offenberg of the U.S. EPA and Allan Biedler, Chris Allen, and James Beilder of CSC for their contributions to this work. This project was supported in part by an appointment to the Internship/Research Participation Program at the Office of Research and Development, U.S. Environmental Protection Agency, administered by the Oak Ridge Institute for Science and Education through an interagency agreement between the U.S. Department of Energy and EPA. PLH and JLJ were partially supported by CARB 11-305 and DOE (BER/ASR) DE-SC0011105.

Disclaimer. Although this work was reviewed by EPA and approved for publication, it may not necessarily reflect official agency policy.

References

Ahmadov, R., McKeen, S., Robinson, A., Bahreini, R., Middlebrook, A., Gouw, J. d., Meagher, J., Hsie, E.-Y., Edgerton, E., Shaw, S., and Trainer, M.: A volatility basis set model for summertime secondary organic aerosols over the eastern United States in 2006, J. Geophys. Res.-Atmos., 117, 2012. 26749

Aiken, A. C., Salcedo, D., Cubison, M. J., Huffman, J. A., DeCarlo, P. F., Ulbrich, I. M., Docherty, K. S., Sueper, D., Kimmel, J. R., Worsnop, D. R., Trimborn, A., Northway, M., Stone, E. A., Schauer, J. J., Volkamer, R. M., Fortner, E., de Foy, B., Wang, J., Laskin, A., Shutthanandan, V., Zheng, J., Zhang, R., Gaffney, J., Marley, N. A., Paredes-Miranda, G.,

ACPD
15, 26745–26793, 2015

Arnott, W. P., Molina, L. T., Sosa, G., and Jimenez, J. L.: Mexico City aerosol analysis during MILAGRO using high resolution aerosol mass spectrometry at the urban supersite (T0) – Part 1: Fine particle composition and organic source apportionment, Atmos. Chem. Phys., 9, 6633–6653, doi:10.5194/acp-9-6633-2009, 2009. 26748

Allan, J. D., Williams, P. I., Morgan, W. T., Martin, C. L., Flynn, M. J., Lee, J., Nemitz, E., Phillips, G. J., Gallagher, M. W., and Coe, H.: Contributions from transport, solid fuel burning and cooking to primary organic aerosols in two UK cities, Atmos. Chem. Phys., 10, 647–668, doi:10.5194/acp-10-647-2010, 2010. 26756

Bahreini, R., Middlebrook, A. M., de Gouw, J. A., Warneke, C., Trainer, M., Brock, C. A., Stark, H., Brown, S. S., Dube, W. P., Gilman, J. B., Hall, K., Holloway, J. S., Kuster, W. C., Perring, A. E., Prevot, A. S. H., Schwarz, J. P., Spackman, J. R., Szidat, S., Wagner, N. L., Weber, R. J., Zotter, P., and Parrish, D. D.: Gasoline emissions dominate over diesel in formation of secondary organic aerosol mass, Geophys. Res. Lett., 39, L06805, doi:10.1029/2011GL050718, 2012. 26748, 26751, 26766

Baker, K. R., Misenis, C., Obland, M. D., Ferrare, R. A., Scarino, A. J., and Kelly, J. T.: Evaluation of surface and upper air fine scale WRF meteorological modeling of the May and June 2010 CalNex period in California, Atmos. Environ., 80, 299–309, 2013. 26752

Baker, K. R., Carlton, A. G., Kleindienst, T. E., Offenberg, J. H., Beaver, M. R., Gentner, D. R., Goldstein, A. H., Hayes, P. L., Jimenez, J. L., Gilman, J. B., de Gouw, J. A., Woody, M. C., Pye, H. O. T., Kelly, J. T., Lewandowski, M., Jaoui, M., Stevens, P. S., Brune, W. H., Lin, Y.-H., Rubitschun, C. L., and Surratt, J. D.: Gas and aerosol carbon in California: comparison of measurements and model predictions in Pasadena and Bakersfield, Atmos. Chem. Phys., 15, 5243–5258, doi:10.5194/acp-15-5243-2015, 2015. 26747, 26748, 26749, 26754, 26761, 26764, 26765, 26767, 26769

Bey, I., Jacob, D. J., Yantosca, R. M., Logan, J. A., Field, B. D., Fiore, A. M., Li, Q., Liu, H. Y., Mickley, L. J., and Schultz, M. G.: Global modeling of tropospheric chemistry with assimilated meteorology: model description and evaluation, J. Geophys. Res.-Atmos., 106, 23073–23095, 2001. 26752

Borbon, A., Gilman, J. B., Kuster, W. C., Grand, N., Chevaillier, S., Colomb, A., Dolgorouky, C., Gros, V., Lopez, M., Sarda-Esteve, R., Holloway, J., Stutz, J., Petetin, H., McKeen, S., Beekmann, M., Warneke, C., Parrish, D. D., and de Gouw, J. A.: Emission ratios of anthropogenic volatile organic compounds in northern mid-latitude megacities: Observations versus emis-

ACPD
15, 26745–26793, 2015

sion inventories in Los Angeles and Paris, J. Geophys. Res.-Atmos., 118, 2041–2057, 2013. 26748

Brioude, J., Angevine, W. M., Ahmadov, R., Kim, S.-W., Evan, S., McKeen, S. A., Hsie, E.-Y., Frost, G. J., Neuman, J. A., Pollack, I. B., Peischl, J., Ryerson, T. B., Holloway, J., Brown, S. S., Nowak, J. B., Roberts, J. M., Wofsy, S. C., Santoni, G. W., Oda, T., and Trainer, M.: Top-down estimate of surface flux in the Los Angeles Basin using a mesoscale inverse modeling technique: assessing anthropogenic emissions of CO, NO_x and CO_2 and their impacts, Atmos. Chem. Phys., 13, 3661–3677, doi:10.5194/acp-13-3661-2013, 2013. 26769

Byun, D. and Schere, K. L.: Review of the governing equations, computational algorithms, and other components of the Models-3 Community Multiscale Air Quality (CMAQ) modeling system, Appl. Mech. Rev., 59, 51–77, 2006. 26748

Carlton, A. G. and Baker, K. R.: Photochemical modeling of the Ozark isoprene volcano: MEGAN, BEIS, and their impacts on air quality predictions, Environ. Sci. Technol., 45, 4438–4445, 2011. 26751

Carlton, A. G., Bhave, P. V., Napelenok, S. L., Edney, E. D., Sarwar, G., Pinder, R. W., Pouliot, G. A., and Houyoux, M.: Model representation of secondary organic aerosol in CMAQv4.7, Environ. Sci. Technol., 44, 8553–8560, 2010. 26749, 26750

Chen, J. and Griffin, R. J.: Modeling secondary organic aerosol formation from oxidation of α-pinene, β-pinene, and d-limonene, Atmos. Environ., 39, 7731–7744, 2005. 26750

Craven, J. S., Metcalf, A. R., Bahreini, R., Middlebrook, A., Hayes, P. L., Duong, H. T., Sorooshian, A., Jimenez, J. L., Flagan, R. C., and Seinfeld, J. H.: Los Angeles Basin airborne organic aerosol characterization during CalNex, J. Geophys. Res.-Atmos., 118, 11453–11467, 2013. 26748

De Gouw, J. and Jimenez, J.: Organic aerosols in the Earth's atmosphere, Environ. Sci. Technol., 43, 7614–7618, 2009. 26762

De Gouw, J., Brock, C., Atlas, E., Bates, T., Fehsenfeld, F., Goldan, P., Holloway, J., Kuster, W., Lerner, B., Matthew, B., Middlebrook, A., Onasch, T., Peltier, R., Quinn, P., Senff, C., Stohl, A., Sullivan, A., Trainer, M., Warneke, C., Weber, R., and Williams, E.: Sources of particulate matter in the northeastern United States in summer: 1. Direct emissions and secondary formation of organic matter in urban plumes, J. Geophys. Res.-Atmos., 113, D08301, doi:10.1029/2007JD009243, 2008. 26760

ACPD
15, 26745–26793, 2015

Docherty, K. S., Stone, E. A., Ulbrich, I. M., DeCarlo, P. F., Snyder, D. C., Schauer, J. J., Peltier, R. E., Weber, R. J., Murphy, S. M., Seinfeld, J. H., Grover, B. D., Eatough, D. J., and Jimenez, J. L.: Apportionment of primary and secondary organic aerosols in southern California during the 2005 Study of Organic Aerosols in Riverside (SOAR-1), Environ. Sci. Technol., 42, 7655–7662, 2008. 26748

Donahue, N., Robinson, A., Stanier, C., and Pandis, S.: Coupled partitioning, dilution, and chemical aging of semivolatile organics, Environ. Sci. Technol., 40, 2635–2643, 2006. 26750

Donahue, N., Chuang, W., Epstein, S., Kroll, J., Worsnop, D., Robinson, A., Adams, P., and Pandis, S.: Why do organic aerosols exist? Understanding aerosol lifetimes using the two-dimensional volatility basis set, Environ. Chem., 10, 151–157, 2013. 26750

Donahue, N. M., Henry, K. M., Mentel, T. F., Kiendler-Scharr, A., Spindler, C., Bohn, B., Brauers, T., Dorn, H. P., Fuchs, H.,Tillmann, R., Wahner, A., Saathoff, H., Naumann, K., Möhler, O., Leisner, T., Müller, L., Rennig, M., Hoffmann, T., Salo, K., Hallquist, M., Frosch, M., Bilde, M., Tritscher, T., Barmet, P., Praplan, A., DeCarlo, P., Dommen, J., Prŕvôt, A., and Baltensperger, U.: Aging of biogenic secondary organic aerosol via gas-phase OH radical reactions, P. Natl. Acad. Sci. USA, 109, 13503–13508, 2012. 26750, 26751, 26770

Dzepina, K., Volkamer, R. M., Madronich, S., Tulet, P., Ulbrich, I. M., Zhang, Q., Cappa, C. D., Ziemann, P. J., and Jimenez, J. L.: Evaluation of recently-proposed secondary organic aerosol models for a case study in Mexico City, Atmos. Chem. Phys., 9, 5681–5709, doi:10.5194/acp-9-5681-2009, 2009. 26749, 26753, 26763

Ensberg, J. J., Hayes, P. L., Jimenez, J. L., Gilman, J. B., Kuster, W. C., de Gouw, J. A., Holloway, J. S., Gordon, T. D., Jathar, S., Robinson, A. L., and Seinfeld, J. H.: Emission factor ratios, SOA mass yields, and the impact of vehicular emissions on SOA formation, Atmos. Chem. Phys., 14, 2383–2397, doi:10.5194/acp-14-2383-2014, 2014. 26748, 26766

Foley, K. M., Roselle, S. J., Appel, K. W., Bhave, P. V., Pleim, J. E., Otte, T. L., Mathur, R., Sarwar, G., Young, J. O., Gilliam, R. C., Nolte, C. G., Kelly, J. T., Gilliland, A. B., and Bash, J. O.: Incremental testing of the Community Multiscale Air Quality (CMAQ) modeling system version 4.7, Geosci. Model Dev., 3, 205–226, doi:10.5194/gmd-3-205-2010, 2010. 26760

Fountoukis, C., Racherla, P. N., Denier van der Gon, H. A. C., Polymeneas, P., Charalampidis, P. E., Pilinis, C., Wiedensohler, A., Dall'Osto, M., O'Dowd, C., and Pandis, S. N.: Evaluation of a three-dimensional chemical transport model (PMCAMx) in the European domain during the EUCAARI May 2008 campaign, Atmos. Chem. Phys., 11, 10331–10347, doi:10.5194/acp-11-10331-2011, 2011. 26750, 26751

ACPD
15, 26745–26793, 2015

Freutel, F., Schneider, J., Drewnick, F., von der Weiden-Reinmüller, S.-L., Crippa, M., Prévôt, A. S. H., Baltensperger, U., Poulain, L., Wiedensohler, A., Sciare, J., Sarda-Estève, R., Burkhart, J. F., Eckhardt, S., Stohl, A., Gros, V., Colomb, A., Michoud, V., Doussin, J. F., Borbon, A., Haeffelin, M., Morille, Y., Beekmann, M., and Borrmann, S.: Aerosol particle measurements at three stationary sites in the megacity of Paris during summer 2009: meteorology and air mass origin dominate aerosol particle composition and size distribution, Atmos. Chem. Phys., 13, 933–959, doi:10.5194/acp-13-933-2013, 2013. 26756

Gentner, D. R., Isaacman, G., Worton, D. R., Chan, A. W. H., Dallmann, T. R., Davis, L., Liu, S., Day, D. A., Russell, L. M., Wilson, K. R., Weber, R., Guha, A., Harley, R. A., and Goldstein, A. H.: Elucidating secondary organic aerosol from diesel and gasoline vehicles through detailed characterization of organic carbon emissions, P. Natl. Acad. Sci. USA, 109, 18318–18323, 2012. 26748, 26766

Grieshop, A. P., Logue, J. M., Donahue, N. M., and Robinson, A. L.: Laboratory investigation of photochemical oxidation of organic aerosol from wood fires 1: measurement and simulation of organic aerosol evolution, Atmos. Chem. Phys., 9, 1263–1277, doi:10.5194/acp-9-1263-2009, 2009. 26759

Hayes, P. L., Ortega, A. M., Cubison, M. J., Froyd, K. D., Zhao, Y., Cliff, S. S., Hu, W. W., Toohey, D. W., Flynn, J. H., Lefer, B. L., Grossberg, N., Alvarez, S., Rappenglück, B., Taylor, J. W., Allan, J. D., Holloway, J. S., Gilman, J. B., Kuster, W. C., de Gouw, J. A., Massoli, P., Zhang, X., Liu, J., Weber, R. J., Corrigan, A. L., Russell, L. M., Isaacman, G., Worton, D. R., Kreisberg, N. M., Goldstein, A. H., Thalman, R., Waxman, E. M., Volkamer, R., Lin, Y. H., Surratt, J. D., Kleindienst, T. E., Offenberg, J. H., Dusanter, S., Griffith, S., Stevens, P. S., Brioude, J., Angevine, W. M., and Jimenez, J. L.: Organic aerosol composition and sources in Pasadena, California, during the 2010 CalNex campaign, J. Geophys. Res.-Atmos., 118, 9233–9257, 2013. 26747, 26748, 26751, 26754, 26756, 26761, 26762, 26764

Hayes, P. L., Carlton, A. G., Baker, K. R., Ahmadov, R., Washenfelder, R. A., Alvarez, S., Rappenglück, B., Gilman, J. B., Kuster, W. C., de Gouw, J. A., Zotter, P., Prévôt, A. S. H., Szidat, S., Kleindienst, T. E., Offenberg, J. H., Ma, P. K., and Jimenez, J. L.: Modeling the formation and aging of secondary organic aerosols in Los Angeles during CalNex 2010, Atmos. Chem. Phys., 15, 5773–5801, doi:10.5194/acp-15-5773-2015, 2015. 26749, 26753, 26759, 26760, 26761, 26763, 26764, 26765, 26766, 26767, 26768, 26789

ACPD
15, 26745–26793, 2015

Henderson, B. H., Akhtar, F., Pye, H. O. T., Napelenok, S. L., and Hutzell, W. T.: A database and tool for boundary conditions for regional air quality modeling: description and evaluation, Geosci. Model Dev., 7, 339–360, doi:10.5194/gmd-7-339-2014, 2014. 26752

Herndon, S. C., Onasch, T. B., Wood, E. C., Kroll, J. H., Canagaratna, M. R., Jayne, J. T., Zavala, M. A., Knighton, W. B., Mazzoleni, C., Dubey, M. K., Ulbrich, I., Jimenez, J., Seila, R., de Gouw, J., de Foy, B., Fast, J., Molina, L., Kolb, C., and Worsnop, D.: Correlation of secondary organic aerosol with odd oxygen in Mexico City, Geophys. Res. Lett., 35, L15804, doi:10.1029/2008GL034058, 2008. 26762

Hersey, S. P., Craven, J. S., Schilling, K. A., Metcalf, A. R., Sorooshian, A., Chan, M. N., Flagan, R. C., and Seinfeld, J. H.: The Pasadena Aerosol Characterization Observatory (PACO): chemical and physical analysis of the Western Los Angeles basin aerosol, Atmos. Chem. Phys., 11, 7417–7443, doi:10.5194/acp-11-7417-2011, 2011. 26748

Hildebrandt, L., Donahue, N. M., and Pandis, S. N.: High formation of secondary organic aerosol from the photo-oxidation of toluene, Atmos. Chem. Phys., 9, 2973–2986, doi:10.5194/acp-9-2973-2009, 2009. 26750

Hodzic, A. and Jimenez, J. L.: Modeling anthropogenically controlled secondary organic aerosols in a megacity: a simplified framework for global and climate models, Geosci. Model Dev., 4, 901–917, doi:10.5194/gmd-4-901-2011, 2011. 26763, 26768

Hodzic, A., Jimenez, J. L., Madronich, S., Canagaratna, M. R., DeCarlo, P. F., Kleinman, L., and Fast, J.: Modeling organic aerosols in a megacity: potential contribution of semi-volatile and intermediate volatility primary organic compounds to secondary organic aerosol formation, Atmos. Chem. Phys., 10, 5491–5514, doi:10.5194/acp-10-5491-2010, 2010. 26753, 26760

Houyoux, M. R., Vukovich, J. M., Coats, C. J., Wheeler, N. J., and Kasibhatla, P. S.: Emission inventory development and processing for the Seasonal Model for Regional Air Quality (SMRAQ) project, J. Geophys. Res.-Atmos., 105, 9079–9090, 2000. 26752

Huang, X.-F., He, L.-Y., Hu, M., Canagaratna, M. R., Sun, Y., Zhang, Q., Zhu, T., Xue, L., Zeng, L.-W., Liu, X.-G., Zhang, Y.-H., Jayne, J. T., Ng, N. L., and Worsnop, D. R.: Highly time-resolved chemical characterization of atmospheric submicron particles during 2008 Beijing Olympic Games using an Aerodyne High-Resolution Aerosol Mass Spectrometer, Atmos. Chem. Phys., 10, 8933–8945, doi:10.5194/acp-10-8933-2010, 2010. 26756

Huffman, J., Docherty, K., Mohr, C., Cubison, M., Ulbrich, I., Ziemann, P., Onasch, T., and Jimenez, J.: Chemically-resolved volatility measurements of organic aerosol from different sources, Environ. Sci. Technol., 43, 5351–5357, 2009. 26753, 26781

ACPD
15, 26745–26793, 2015

Jathar, S. H., Gordon, T. D., Hennigan, C. J., Pye, H. O. T., Pouliot, G., Adams, P. J., Donahue, N. M., and Robinson, A. L.: Unspeciated organic emissions from combustion sources and their influence on the secondary organic aerosol budget in the United States, P. Natl. Acad. Sci. USA, 111, 10473–10478, 2014. 26748, 26763, 26770

Kelly, J. T., Baker, K. R., Nowak, J. B., Murphy, J. G., Markovic, M. Z., VandenBoer, T. C., Ellis, R. A., Neuman, J. A., Weber, R. J., Roberts, J. M.,, Veres, P. R., de Gouw, J. A., Beaver, M. R., Newman, S., and Misenis, C.: Fine-scale simulation of ammonium and nitrate over the South Coast Air Basin and San Joaquin Valley of California during CalNex-2010, J. Geophys. Res.-Atmos., 119, 3600–3614, 2014. 26762

Kleinman, L. I., Springston, S. R., Daum, P. H., Lee, Y.-N., Nunnermacker, L. J., Senum, G. I., Wang, J., Weinstein-Lloyd, J., Alexander, M. L., Hubbe, J., Ortega, J., Canagaratna, M. R., and Jayne, J.: The time evolution of aerosol composition over the Mexico City plateau, Atmos. Chem. Phys., 8, 1559–1575, doi:10.5194/acp-8-1559-2008, 2008. 26761

Koo, B., Knipping, E., and Yarwood, G.: 1.5-dimensional volatility basis set approach for modeling organic aerosol in CAMx and CMAQ, Atmos. Environ., 95, 158–164, 2014. 26749, 26750, 26751

Lane, T. E., Donahue, N. M., and Pandis, S. N.: Simulating secondary organic aerosol formation using the volatility basis-set approach in a chemical transport model, Atmos. Environ., 42, 7439–7451, 2008. 26750

May, A. A., Levin, E. J., Hennigan, C. J., Riipinen, I., Lee, T., Collett, J. L., Jimenez, J. L., Kreidenweis, S. M., and Robinson, A. L.: Gas-particle partitioning of primary organic aerosol emissions: 3. Biomass burning, J. Geophys. Res.-Atmos., 118, 11–327, 2013a. 26781

May, A. A., Presto, A. A., Hennigan, C. J., Nguyen, N. T., Gordon, T. D., and Robinson, A. L.: Gas-particle partitioning of primary organic aerosol emissions: 1. Gasoline vehicle exhaust, Atmos. Environ., 77, 128–139, 2013b. 26781

May, A. A., Presto, A. A., Hennigan, C. J., Nguyen, N. T., Gordon, T. D., and Robinson, A. L.: Gas-particle partitioning of primary organic aerosol emissions: 2. Diesel vehicles, Environ. Sci. Technol., 47, 8288–8296, 2013c. 26781

Mohr, C., DeCarlo, P. F., Heringa, M. F., Chirico, R., Slowik, J. G., Richter, R., Reche, C., Alastuey, A., Querol, X., Seco, R., Peñuelas, J., Jiménez, J. L., Crippa, M., Zimmermann, R., Baltensperger, U., and Prévôt, A. S. H.: Identification and quantification of organic aerosol from cooking and other sources in Barcelona using aerosol mass spectrometer data, Atmos. Chem. Phys., 12, 1649–1665, doi:10.5194/acp-12-1649-2012, 2012. 26756

ACPD
15, 26745–26793, 2015

Morino, Y., Tanabe, K., Sato, K., and Ohara, T.: Secondary organic aerosol model intercomparison based on secondary organic aerosol to odd oxygen ratio in Tokyo, J. Geophys. Res.-Atmos., 119, 13489–13505, 2014. 26762

Murphy, B. N. and Pandis, S. N.: Simulating the formation of semivolatile primary and secondary organic aerosol in a regional chemical transport model, Environ. Sci. Technol., 43, 4722–4728, 2009. 26750

Pfister, G., Emmons, L., Hess, P., Lamarque, J.-F., Orlando, J., Walters, S., Guenther, A., Palmer, P., and Lawrence, P.: Contribution of isoprene to chemical budgets: A model tracer study with the NCAR CTM MOZART-4, J. Geophys. Res.-Atmos., 113, D05308, doi:10.1029/2007JD008948, 2008. 26750

Pye, H. O. T. and Seinfeld, J. H.: A global perspective on aerosol from low-volatility organic compounds, Atmos. Chem. Phys., 10, 4377–4401, doi:10.5194/acp-10-4377-2010, 2010. 26750, 26759

Robinson, A. L., Donahue, N. M., Shrivastava, M. K., Weitkamp, E. A., Sage, A. M., Grieshop, A. P., Lane, T. E., Pierce, J. R., and Pandis, S. N.: Rethinking organic aerosols: Semivolatile emissions and photochemical aging, Science, 315, 1259–1262, 2007. 26749, 26751, 26752, 26753, 26759, 26760, 26763, 26781

Ryerson, T. B., Andrews, A. E., Angevine, W. M., Bates, T. S., Brock, C. A., Cairns, B., Cohen, R. C., Cooper, O. R., de Gouw, J. A., Fehsenfeld, F. C., Ferrare, R. A., Fischer, M. L., Flagan, R. C., Goldstein, A. H., Hair, J. W., Hardesty, R. M., Hostetler, C. A., Jimenez, J. L., Langford, A. O., McCauley, E., McKeen, S. A., Molina, L. T., Nenes, A., Oltmans, S. J., Parrish, D. D., Pederson, J. R., Pierce, R. B., Prather, K., Quinn, P. K., Seinfeld, J. H., Senff, C. J., Sorooshian, A., Stutz, J., Surratt, J. D., Trainer, M., Volkamer, R., Williams, E. J., and Wofsy, S. C.: The 2010 California Research at the Nexus of Air Quality and Climate Change (CalNex) field study, J. Geophys. Res.-Atmos., 118, 5830–5866, 2013. 26747, 26754

Shrivastava, M., Fast, J., Easter, R., Gustafson Jr., W. I., Zaveri, R. A., Jimenez, J. L., Saide, P., and Hodzic, A.: Modeling organic aerosols in a megacity: comparison of simple and complex representations of the volatility basis set approach, Atmos. Chem. Phys., 11, 6639–6662, doi:10.5194/acp-11-6639-2011, 2011. 26753, 26760

Simon, H. and Bhave, P. V.: Simulating the ree of oxidation in atmospheric organic particles, Environ. Sci. Technol., 46, 331–339, 2012. 26748

ACPD
15, 26745–26793, 2015

Skamarock, W. C. and Klemp, J. B.: A time-split nonhydrostatic atmospheric model for weather research and forecasting applications, J.Comput. Phys., 227, 3465–3485, 2008. 26752
Sun, Y.-L., Zhang, Q., Schwab, J. J., Demerjian, K. L., Chen, W.-N., Bae, M.-S., Hung, H.-M., Hogrefe, O., Frank, B., Rattigan, O. V., and Lin, Y.-C.: Characterization of the sources and processes of organic and inorganic aerosols in New York city with a high-resolution time-of-flight aerosol mass apectrometer, Atmos. Chem. Phys., 11, 1581–1602, doi:10.5194/acp-11-1581-2011, 2011. 26756
Tsimpidi, A. P., Karydis, V. A., Zavala, M., Lei, W., Molina, L., Ulbrich, I. M., Jimenez, J. L., and Pandis, S. N.: Evaluation of the volatility basis-set approach for the simulation of organic aerosol formation in the Mexico City metropolitan area, Atmos. Chem. Phys., 10, 525–546, doi:10.5194/acp-10-525-2010, 2010. 26753
US Environmental Protection Agency: 2011 National Emission Inventory, 2014a. 26751
US Environmental Protection Agency: North American Emissions Inventories – Mexico, 2014b. 26751
Volkamer, R., Jimenez, J. L., San Martini, F., Dzepina, K., Zhang, Q., Salcedo, D., Molina, L. T., Worsnop, D. R., and Molina, M. J.: Secondary organic aerosol formation from anthropogenic air pollution: rapid and higher than expected, Geophys. Res. Lett., 33, L17811, doi:10.1029/2006GL026899, 2006. 26760
Wood, E. C., Canagaratna, M. R., Herndon, S. C., Onasch, T. B., Kolb, C. E., Worsnop, D. R., Kroll, J. H., Knighton, W. B., Seila, R., Zavala, M., Molina, L. T., DeCarlo, P. F., Jimenez, J. L., Weinheimer, A. J., Knapp, D. J., Jobson, B. T., Stutz, J., Kuster, W. C., and Williams, E. J.: Investigation of the correlation between odd oxygen and secondary organic aerosol in Mexico City and Houston, Atmos. Chem. Phys., 10, 8947–8968, doi:10.5194/acp-10-8947-2010, 2010. 26762
Yarwood, G., Rao, S., Yocke, M., and Whitten, G. Z.: Updates to the Carbon Bond chemical Mechanism: CB05, ENVIRON International Corporation, Novato, CA, 2005. 26749
Zhang, Q., Jimenez, J. L., Canagaratna, M. R., Allan, J. D., Coe, H., Ulbrich, I., Alfarra, M. R., Takami, A., Middlebrook, A. M., Sun, Y. L., Dzepina, K., Dunlea, E., Docherty, K., DeCarlo, P. F., Salcedo, D., Onasch, T., Jayne, J. T., Miyoshi, T., Shimono, A., Hatakeyama, S., Takegawa, N., Kondo, Y., Schneider, J., Drewnick, F., Borrmann, S., Weimer, S., Demerjian, K., Williams, P., Bower, K., Bahreini, R., Cottrell, L., Griffin, R. J., Rautiainen, J., Sun, J. Y., Zhang, Y. M., and Worsnop, D. R.: Ubiquity and dominance of oxygenated species

ACPD
15, 26745–26793, 2015

in organic aerosols in anthropogenically-influenced Northern Hemisphere midlatitudes, Geophys. Res. Lett., 34, L13801, doi:10.1029/2007GL029979, 2007. 26748

Zhang, Q. J., Beekmann, M., Freney, E., Sellegri, K., Pichon, J. M., Schwarzenboeck, A., Colomb, A., Bourrianne, T., Michoud, V., and Borbon, A.: Formation of secondary organic aerosol in the Paris pollution plume and its impact on surrounding regions, Atmos. Chem. Phys. Discuss., 15, 8073–8111, doi:10.5194/acpd-15-8073-2015, 2015. 26762

Zhang, X., Cappa, C. D., Jathar, S. H., McVay, R. C., Ensberg, J. J., Kleeman, M. J., and Seinfeld, J. H.: Influence of vapor wall loss in laboratory chambers on yields of secondary organic aerosol, P. Natl. Acad. Sci. USA, 111, 5802–5807, 2014. 26748, 26763, 26767, 26770

Zhao, Y., Hennigan, C. J., May, A. A., Tkacik, D. S., de Gouw, J. A., Gilman, J. B., Kuster, W., Borbon, A., and Robinson, A. L.: Intermediate-volatility organic compounds: a large source of secondary organic aerosol, Environ. Sci. Technol., 48, 13743–13750, 2014. 26771

Zotter, P., El-Haddad, I., Zhang, Y. L., Hayes, P. L., Zhang, X. L., Lin, Y. H., Wacker, L., Schnelle-Kreis, J., Abbaszade, G., Zimmermann, R., Surratt, J. D., Weber, R., Jimenez, J. L., Szidat, S., Baltensperger, U., and Prevot, A.: Diurnal cycle of fossil and nonfossil carbon using radiocarbon analyses during CalNex, J. Geophys. Res.-Atmos., 119, 6818–6835, 2014. 26747, 26748, 26757, 26764, 26765

ACPD
15, 26745–26793, 2015

Table 1. CMAQ-VBS volatility distribution of POA emissions from gasoline vehicles, diesel vehicles, biomass burning, nonvolatile (e.g. fugitive dust), meat cooking, and "other" sources.

Source	Non-Vol[a]	10^0	10^1	10^2	10^3
Gas Vehicles (GV)[b]	0.27	0.15	0.26	0.15	0.17
Diesel Vehicles (DV)[c]	0.03	0.25	0.37	0.24	0.11
Biomass Burning (BB)[d]	0.20	0.10	0.10	0.20	0.40
Nonvolatile (NV)	1.00	0.00	0.00	0.00	0.00
Meat Cooking (MC)[e]	0.35	0.35	0.10	0.10	0.10
Other (OP)[f]	0.09	0.09	0.14	0.18	0.50

[a] Nonvolatile bin represents C^* values of 10^{-2} and 10^{-1} $\mu g m^{-3}$.
[b] May et al. (2013b).
[c] May et al. (2013c).
[d] May et al. (2013a).
[e] Estimated from Huffman et al. (2009).
[f] Robinson et al. (2007).

ACPD
15, 26745–26793, 2015

Table 2. Domain and modeling period (4 May to 30 June 2010) total NEI POA emissions (tons) for gasoline vehicles, diesel vehicles, biomass burning, nonvolatile (e.g. fugitive dust), meat cooking, and "other" sources.

Source	Emissions (t)
Gas Vehicles (GV)	1990
Diesel Vehicles (DV)	800
Biomass Burning (BB)	8550
Nonvolatile (NV)	540
Meat Cooking (MC)	1470
Other (OP)	2070

ACPD
15, 26745–26793, 2015

Table 3. CMAQ-VBS organic carbon (OC) and elemental carbon (EC) model predictions evaluated against routine modeling network sites in the modeling domain (IMPROVE and CSN). Evaluation metrics include median bias (MdnB), median error (MdnE), normalized median bias (NMdnB), and normalized median error (NMdnE).

Species	Network	Mean Obs. ($\mu g\,m^{-3}$)	Mean Model ($\mu g\,m^{-3}$)	MdnB ($\mu g\,m^{-3}$)	MdnE ($\mu g\,m^{-3}$)	NMdnB (%)	NMdnE (%)
OC	IMPROVE (247)	0.71	0.23	−0.38	0.38	−63.9	64.6
	CSN (159)	1.26	0.75	−0.31	0.44	−25.5	36.5
EC	IMPROVE (249)	0.10	0.09	−0.02	0.03	−20.3	40.8
	CSN (159)	0.33	0.58	0.24	0.26	81.4	87.7

ACPD
15, 26745–26793, 2015

Table 4. As in Table 3 but for CMAQ-VBS organic carbon (OC) model predictions in sensitivity simulations with aging of biogenic SOA.

Species	Network	Mean Obs. ($\mu g\,m^{-3}$)	Mean Model ($\mu g\,m^{-3}$)	MdnB ($\mu g\,m^{-3}$)	MdnE ($\mu g\,m^{-3}$)	NMdnB (%)	NMdnE (%)
OC	IMPROVE (247)	0.71	0.42	−0.25	0.27	−41.8	45.0
	CSN (159)	1.26	1.00	−0.16	0.37	−13.4	30.6

ACPD
15, 26745–26793, 2015

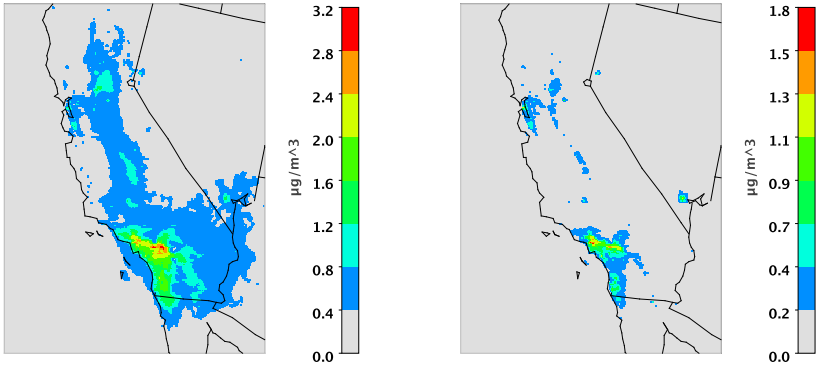

(a) Total OA (b) POA

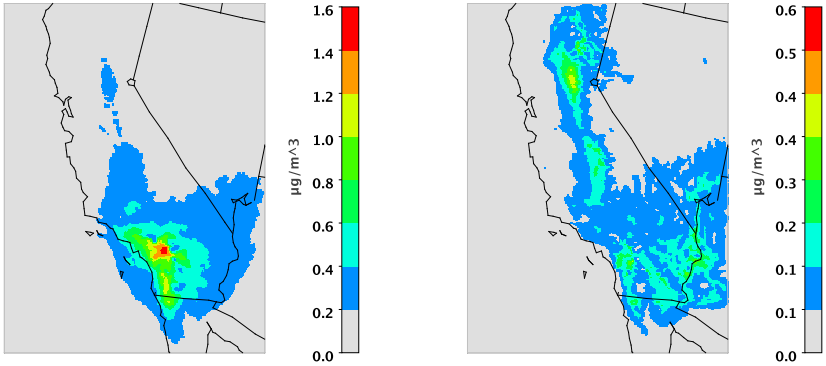

(c) Anthropogenic SOA (d) Biogenic SOA

Figure 1. CMAQ-VBS modeling period average (15 May to 30 June 2010) concentrations of total OA **(a)**, primary organics **(b)**, anthropogenic SOA **(c)**, and biogenic SOA **(d)**. Note each plot uses a unique scale.

ACPD
15, 26745–26793, 2015

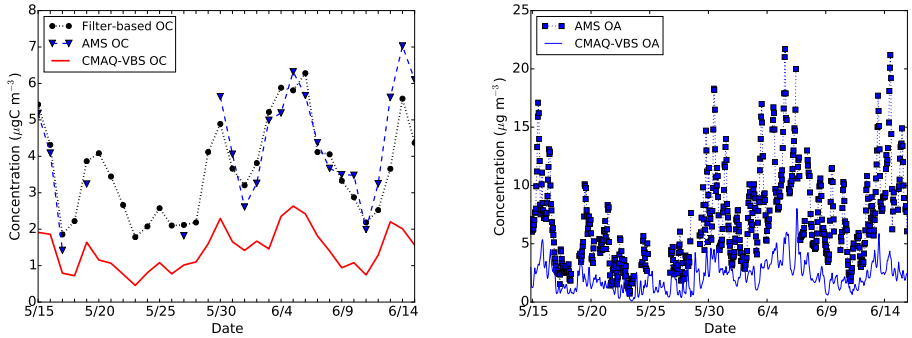

(a) 23-hour average OC (b) Hourly OA

Figure 2. (a) 23 h average modeled and measured (EPA filter-based and AMS) OC and **(b)** hourly modeled and AMS measured OA at Pasadena. AMS measurements in **(a)** include only days with > 16 hourly measurements.

ACPD
15, 26745–26793, 2015

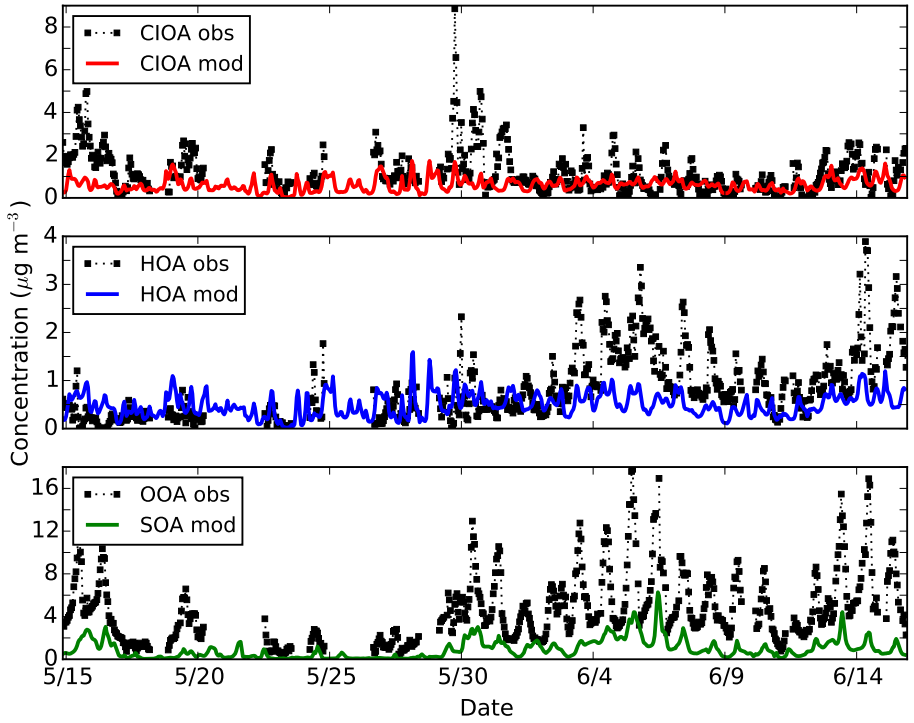

Figure 3. Hourly AMS measured (CIOA obs) and CMAQ-VBS predicted (CIOA mod) meat cooking POA (top), hydrocarbon-like OA (HOA) and POA (middle), and OOA (SV-OOA + LV-OOA) and SOA (bottom) at Pasadena.

ACPD
15, 26745–26793, 2015

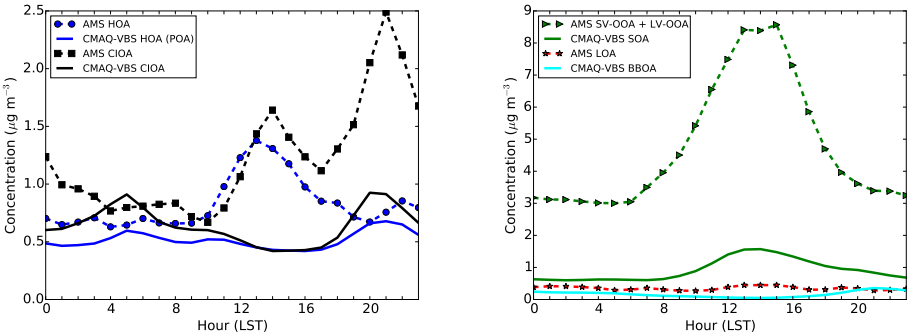

(a) Primary-like (b) Secondary/OOA-like

Figure 4. Diurnal profile of CMAQ-VBS modeled and AMS measured PMF OA components at Pasadena.

ACPD
15, 26745–26793, 2015

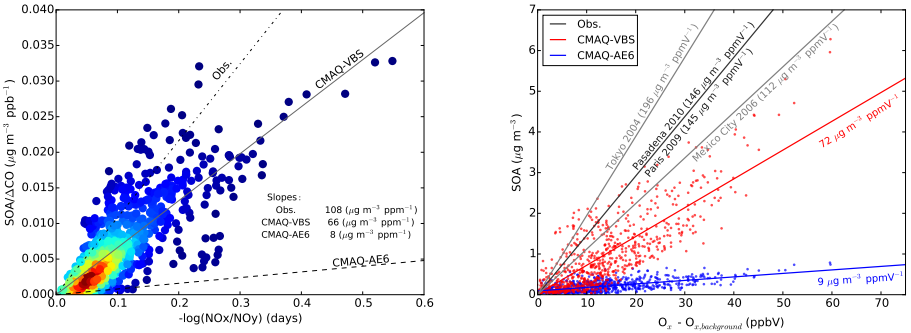

Figure 5. Left: CMAQ-VBS modeled SOA/ΔCO vs. photochemical age [$-\log(NO_x/NO_y)$] at Pasadena. Colors indicate the relative density of points determined using the Gaussian density kernel estimate (red corresponds to high density and blue corresponds to low density). Also indicated are the slopes of the best fit lines for the same metric for observations (Hayes et al., 2015), CMAQ-VBS, and traditional CMAQ (CMAQ-AE6). Right: CMAQ-VBS and CMAQ-AE6 SOA vs. O_x ($O_3 + NO_2$) minus O_x background at Pasadena. Also plotted are the slopes of the best fit line for the same metric for observations made from a number of urban areas, including Pasadena.

ACPD
15, 26745–26793, 2015

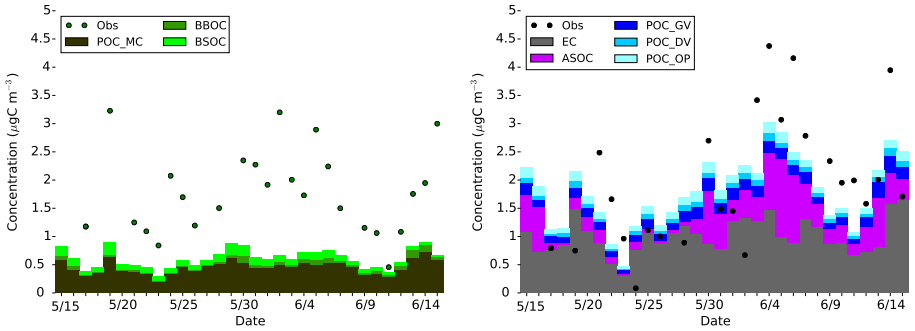

(a) Non-fossil Carbon (b) Fossil Carbon

Figure 6. Daily average CMAQ-VBS **(a)** non-fossil and **(b)** fossil carbon at Pasadena. Non-fossil carbon model species include primary organic carbon from meat cooking (POC_MC), biomass burning OC (BBOC), and biogenic secondary OC (BSOC) while fossil carbon model species include elemental carbon (EC), anthropogenic secondary OC (ASOC), and primary organic carbon from gasoline vehicles (POC_GV), diesel vehicles (POC_DV), and other sources (POC_OP).

ACPD
15, 26745–26793, 2015

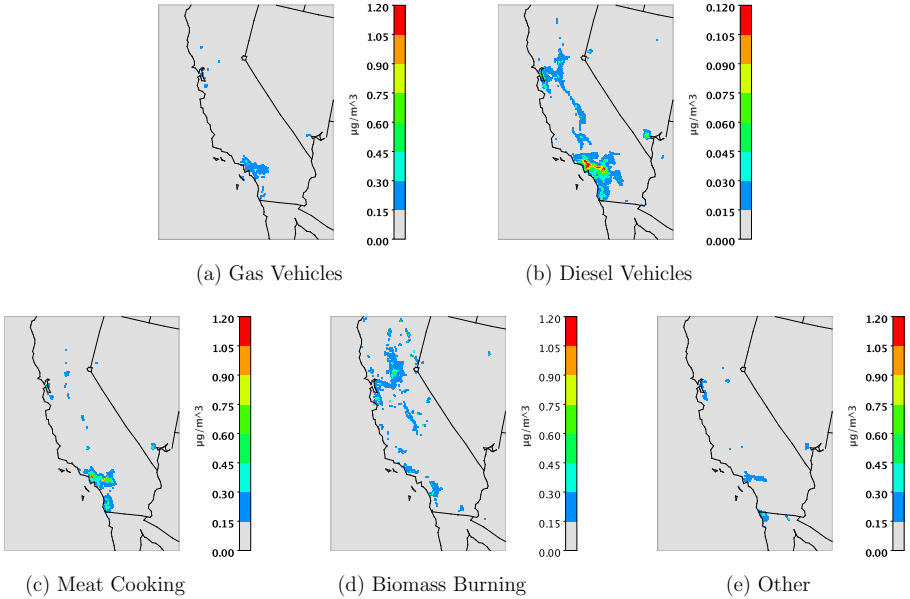

(a) Gas Vehicles (b) Diesel Vehicles

(c) Meat Cooking (d) Biomass Burning (e) Other

Figure 7. CMAQ-VBS modeled primary OA concentrations from gasoline vehicles **(a)**, diesel vehicles **(b)**, meat cooking **(c)**, biomass burning **(d)**, and "other" sources **(e)**. Note the scale for diesel vehicles is an order of magnitude lower than for other sources.

ACPD
15, 26745–26793, 2015

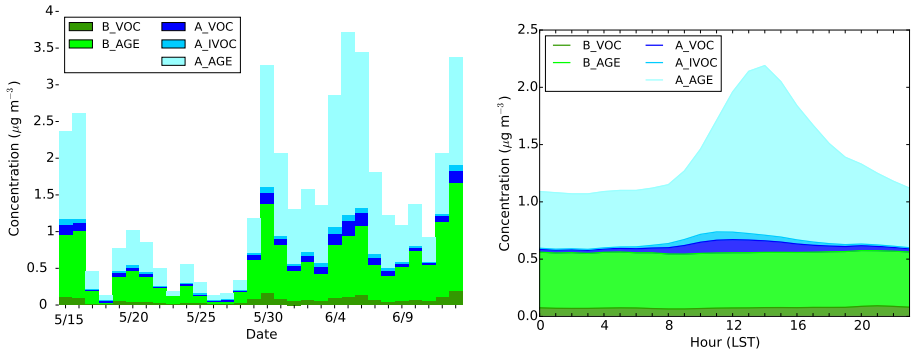

(a) Daily Average (b) Diurnal Profile

Figure 8. Model contributions of anthropogenic and biogenic VOCs (A_VOC, B_VOC), anthropogenic and biogenic IVOCs (A_IVOC, B_IVOC), and aging reactions of anthropogenic and biogenic SVOCs (A_AGE, B_AGE) (originating from both VOCs and IVOCs) to SOA at Pasadena. Note, the aging of biogenic SVOCs was turned on only during sensitivity simulations.

ACPD
15, 26745–26793, 2015

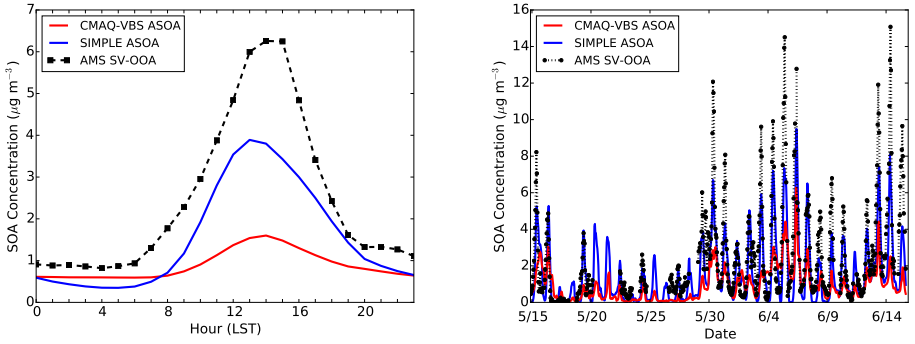

(a) Diurnal Profile (b) All Hours

Figure 9. Comparison of the SIMPLE SOA parameterization in CMAQ to CMAQ-VBS SOA and AMS OOA **(a)** diurnal cycle and **(b)** all hours at the Pasadena CalNex site.

ACPD
15, 26745–26793, 2015